

## C-10-4 CROSS-POLARIZED RADAR RETURN FROM ROUGH SOIL SURFACE

Haruto Hiroswa      Yukihiro Matsuzaka      Shu Yamamoto

Institute of Space and Aeronautical Science  
University of Tokyo, Tokyo, Japan

### 1. Introduction

Scattering on the surface of terrain generally causes radar return to depolarize. The amplitude of cross-polarized electric field component depends on geometric and electric properties of surface media. So we can expect useful information about terrain from cross-polarized radar return as well as like-polarized one.

In recent years many experimental studies have been made to examine radar return from soil surfaces. The effects of soil moisture differences were especially well examined (Ref. 1,2,3). Most of these studies, however, were on the characteristics of like-polarized returns. As to the cross-polarized returns, the dependence on moisture content variations was examined at X-band in our previous studies (Ref. 4,5) and the mechanism of the depolarization was investigated (Ref. 5).

This paper presents results of laboratory measurements of radar return from rough soil surfaces at two frequencies, 4.2 and 9.1 GHz. The analysis of the measurement results suggests that multiple scattering on rough soil surface is principally responsible for the generation of cross-polarized radar returns at 4 GHz as well as 9 GHz. In addition, the measurements suggest the usefulness of cross-polarized radar return for sensitive remote detection of soil moisture.

### 2. Experimental Results

Radar backscatter measurements were made on the bare soil targets equipped within the laboratory. Scattering coefficients of rough soil surfaces were measured as a function of moisture content at 4.2 GHz and 9.1 GHz. Both 4 GHz and 9 GHz scatterometers were designed so as to measure like- and cross-polarized radar backscatter simultaneously. The radars use three horn-antennas mounted parallel on the same platform. The combinations of polarizations are HH (horizontal transmit, horizontal receive) and HV (horizontal transmit, vertical receive). The -3 dB angular widths of the product gain of the antennas are as follows:

- |             |    |                                      |
|-------------|----|--------------------------------------|
| I. 4.2 GHz  | HH | 16° in elevation and 14° in azimuth, |
|             | HV | 18° in elevation and 15° in azimuth, |
| II. 9.1 GHz | HH | 15° in elevation and 17° in azimuth, |
|             | HV | 17° in elevation and 15° in azimuth. |

The modulation of the transmitted waves are AM. The receiving circuits consist of a square-law crystal detector, an amplifier and a phase sensitive detector. The external calibrations of the systems were made by using a corner reflector.

Radar backscatter data were acquired from the bare soil target of three different surface roughness. The three states of surface roughness are designated by A, B and C. The surface roughness is specified by  $\delta$  and L ( See Fig. 1 and 2), where  $\delta$  is a root-mean-square height variation and L is a mean distance between adjacent zero-cross points in an arbitrary surface profile (Ref. 5).

The soil target was on a rotating cart of 2 m square. The thickness of the soil was 20 cm. The soil is classified as loam, named Kanto loam, which is widely distributed in the Kanto district of Japan.

In the measurements, the targets were sprinkled with water, and the soil moisture content was varied, step by step, from a low moisture level to a high moisture one. The antennas of 4 GHz and 9 GHz system were at a height of 1.5 m and 1.3 m, respectively. Backscatter signals were recorded while the cart was being rotated with the angular velocity of about 0.05 rad/sec. Fluctuations due to fading were greatly reduced by the integration (300 msec) in the phase sensitive detector. Number of samples averaged in the calculation of a scattering coefficient was about 60.

Figure 1 and 2 show the measurement results at 4.2 GHz and 9.1 GHz, respectively. The HH and HV scattering coefficient ( $\sigma_{HH}^0$  and  $\sigma_{HV}^0$ ) are given as a function of soil moisture content. The incident angle of radar beam was 30°. The moisture content is a percent of dry soil weight, i.e. a percent ratio of liquid weight to dry soil weight. The average moisture contents were measured on the top 5 cm of soil for 4.2 GHz and on the top 2 cm of soil for 9.1 GHz.

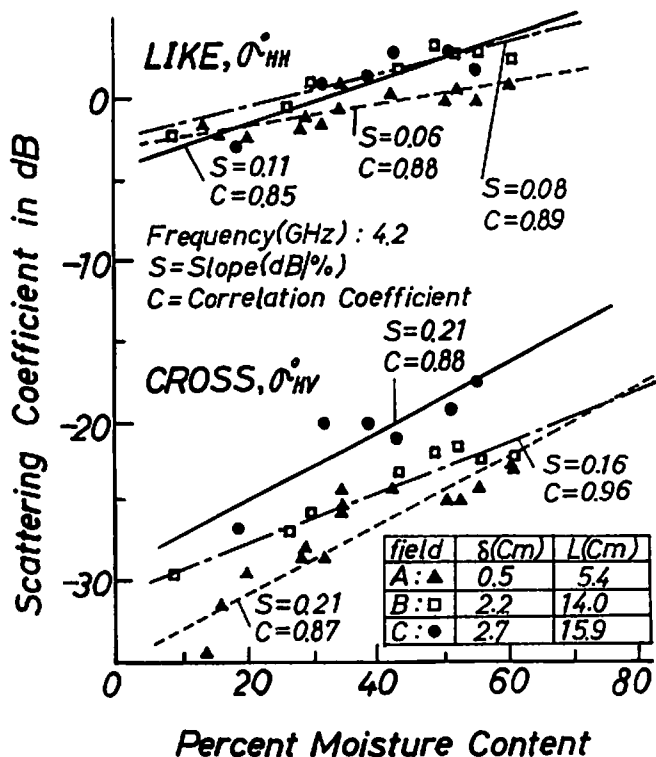


Figure 1. HH and HV scattering coefficients as a function of moisture content at 4.2 GHz.

The results in Fig. 2 (for 9.1 GHz) are fairly similar to the measurement results (at 9.0 GHz) reported in Ref. 4 and 5. Furthermore the comparison of Fig. 1 and 2 shows that the effect of the difference in the frequency was not significant in these experiments. The two figures show that there is general trend of linear increase in scattering coefficient with increase in moisture content and their correlations are fairly high. And the remarkable fact is the  $\sigma_{HV}^0$  has a much higher dependence on moisture content, compared to  $\sigma_{HH}^0$ , at 4.2 GHz as well as at 9.1 GHz. The slopes of the linear regression lines in the figures indicate that the sensitivity to soil moisture content of  $\sigma_{HV}^0$  is about three times, in decibel, as large as that of  $\sigma_{HH}^0$ , at both frequencies.

The effect of the difference of the surface roughness is also not significant in these results, though it seems that as to  $\sigma_{HV}^0$  the slope of the linear regression line of the smooth surface (A) data is slightly larger than those of the rough surface (B and C) data, at both frequencies.

### 3. Discussions on the Mechanism of Depolarization

We reconstruct Fig. 1 and 2 by replacing the moisture content with the power reflection coefficient at a plane soil-air interface for the vertical incidence. This is the same procedure as used in the analyses in Ref. 4 and 5. The power reflection coefficients were calculated using the complex dielectric constants measured on Kanto loam (Ref. 4). The reconstructed figure is Fig. 3, where only linear regression relations, along with the power dependences, are given.

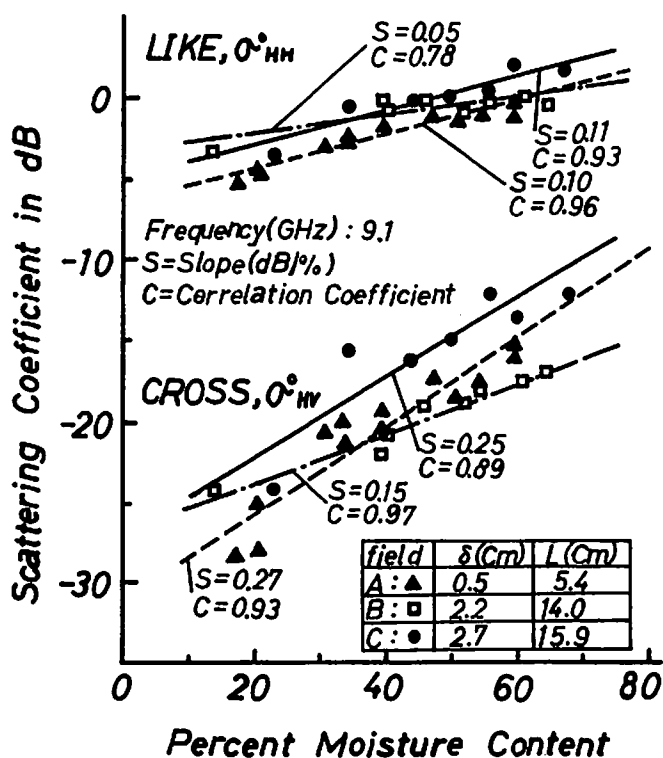


Figure 2. HH and HV scattering coefficients as a function of moisture content at 9.1 GHz.

Figure 3 shows that HV back scattering power (in linear scale) has a dependency of  $\Gamma^{1.2-1.6}$  at 4.2 GHz and  $\Gamma^{1.2-2.2}$  at 9.1 GHz, where  $\Gamma$  is the absolute value (not in decibel) of the power reflection coefficient, and that the power of  $\Gamma$  dependence of HH scattering coefficients is less than one.

The important fact is that the power of  $\Gamma$  dependence of the cross-polarized backscatter is larger than 1, actually near 2 in the most cases. This is nearly the same results as obtained in Ref. 5. So we may conclude that the multiple scattering at soil-air interfaces (scattering twice may be the most important process) is a main mechanism to produce cross-polarized radar returns at C band as well as at X band.

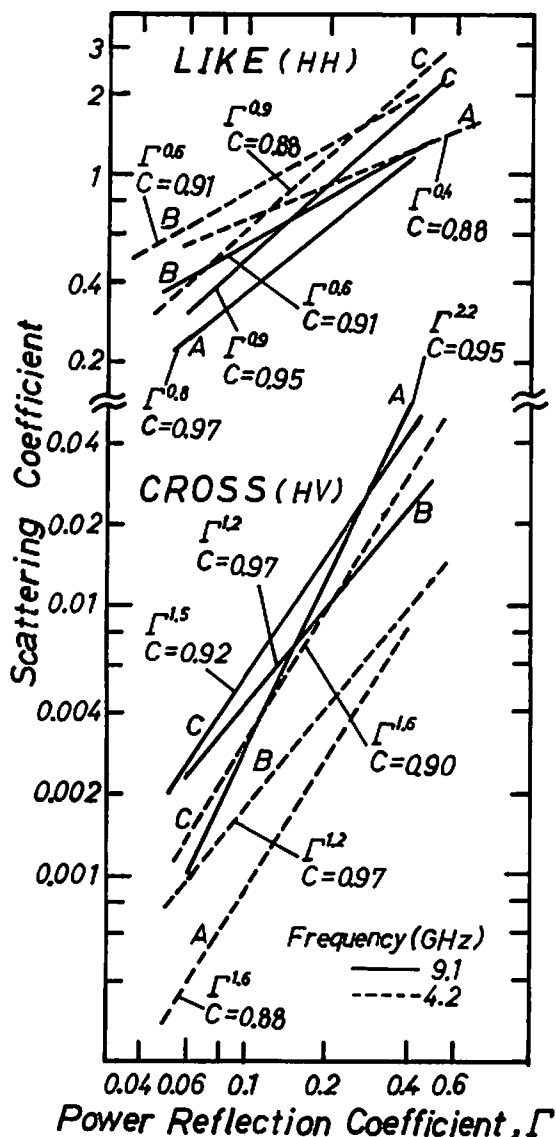


Figure 3. Scattering coefficient versus power reflection coefficient.

#### 4. Conclusions

Measurements on the depolarization of radar return from rough soil surface have shown that the cross-polarized radar return had a higher moisture content sensitivity, compared to the like-polarized return, at 4.2 GHz as well as at 9.1 GHz. The analysis of the data suggests that the main mechanism in producing cross-polarized radar return from rough soil surface at C and X band is multiple scattering at a soil-air interface.

#### Acknowledgment

The authors wish to thank S. Ohtsuka for fabricating the experimental devices.

#### References

1. Dickey, F. M., IEEE Trans on Geoscience Electronics GE-12, 19-22, 1974.
2. Ulaby, F. T., IEEE Trans on Antennas and Propagation AP-22, 257-265, 1974.
3. Ulaby, F. T., et al., Remote Sensing of Environment 3, 185-203, 1974.
4. Hiroswa, H., S. Komiyama, and Y. Matsuzaka, Remote Sensing of Environment 7, 1978 (to be published).
5. Hiroswa, H., S. Komiyama, and Y. Matsuzaka, Int. Conf. on Earth Observation from Space and Management of Planetary Resources, Toulouse, March 1978.